Hydrogen and deuterium site separation in fcc-based mixed-isotope rare-earth hydrides

T. J. Udovic, Q. Huang,* and J. J. Rush
NIST Center for Neutron Research, National Institute of Standards and Technology, 100 Bureau Drive, MS 8562, Gaithersburg, Maryland 20899-8562
(Received 8 October 1999)

The structural arrangements and optic-vibrational densities of states of H and D in various fcc-based, mixed-isotope, rare-earth hydrides as measured by neutron powder diffraction and neutron vibrational spectroscopy clearly indicate preferential isotopic occupation of H in the octahedral interstices and D in the tetrahedral interstices. Although lessened by entropic contributions at high temperature, the degree of isotopic separation increases with decreasing temperature, presumably driven by the differences in the zero-point energies of H and D in the different interstitial sites. Decreasing the temperature below ≈150 K leads to a ''freezing in'' of the H and D lattice configuration prevalent near this temperature, kinetically precluding the complete isotopic site separation expected at temperatures approaching 0 K.

INTRODUCTION

The metal sublattice of the fcc-based rare-earth hydrides possesses two types of interstices to accommodate hydrogen, the more energetically favorable tetrahedral (*t*) sites and the relatively larger yet more weakly absorbing octahedral (*o*) sites. Hydride formation proceeds first by reaction of two hydrogens per metal atom to form the stoichiometric rare-earth dihydride, completely filling the *t* sites. Superstoichiometric dihydrides are formed by the addition to the *o*-site sublattice of up to one more hydrogen per metal atom. The different interstitial sizes and hydrogen-absorption potentials for these two sites leads to significant differences in their respective optic-vibrational energies.[1] For example, in LaH_{2+x},[2] fundamental (i.e., $\nu=0\rightarrow1$) vibrational-energy bands associated with *o*-site H (H_o) atoms are centered near 70 meV, well-separated from the *t*-site H (H_t) bands located above 90 meV. Deuterided analogs display similar vibrational bands downshifted in energy by about a factor of $1/\sqrt{2}$ as expected for the largely harmonic vibrations of the doubly massive D atoms.[3,4]

The marked differences in the vibrational energies associated with the different interstitial sites can lead to interesting isotope effects in mixed-isotope hydrides. In particular, Somenkov *et al.*[5] reported neutron diffraction evidence for unequal H/D isotopic ratios in the *t*-site and *o*-site sublattices of $Ce(H_{0.33}D_{0.67})_3$. This nonrandom distribution represented an isotopic arrangement that reduced the total energy of all local vibrations. In light of this earlier work, we have used neutron scattering methods to investigate the location and dynamics of H and D atoms in a variety of mixed-isotope rare-earth hydrides. In particular, we present in this paper both neutron powder diffraction (NPD) and neutron vibrational spectroscopy (NVS) results that corroborate temperature-dependent D_t and H_o isotopic enrichments in the fcc-based (β-phase) rare-earth hydride $La(H_yD_{1-y})_{2.50}$ over a wide range of H isotopic fraction ($0\leqslant y\leqslant1$), qualitatively consistent with the earlier observations for $Ce(H_{0.33}D_{0.67})_3$.[5] Related measurements on $Tb(H_{0.1}D_{0.9})_{2.22}$ confirm this as a general trend for fcc-based, mixed-isotope, rare-earth hydrides over a wide range of vacancy concentrations.

THEORY

Over the temperature range considered in the present study (≤400 K), the relatively high vibrational-energy levels for the absorbed H and D atoms in these mixed-isotope hydride systems preclude any significant population of the excited-state levels, and the majority of H and D oscillators will be in their ground-state levels. Ignoring, for the moment, phonon dispersion effects due to hydrogen-hydrogen interactions, the *t* and *o* site symmetries result in discrete triply degenerate vibrational levels. Considering the differences in zero-point energies between H and D Einstein oscillators in the three-dimensional lattice, the vibrational-energy change $\Delta E_{\rm vib}$ in the system due to the transposition of one *t*-site H atom and one *o*-site D atom is described by[5]

$$\Delta E_{\rm vib}=\frac{3}{2}\hbar\{(\omega_{\rm H}^{o}+\omega_{\rm D}^{t})-(\omega_{\rm H}^{t}+\omega_{\rm D}^{o})\}, \tag{1}$$

where $\omega_{\rm H}$ and $\omega_{\rm D}$ are the fundamental vibrational frequencies of the H and D atoms, respectively, and the superscripts denote the sublattice. [It should be noted that Eq. (1) is still valid if one includes phonon dispersion effects by defining $\omega_{\rm H}$ and $\omega_{\rm D}$ as density-of-states-weighted mean fundamental frequencies $\overline{\omega}_{\rm H}$ and $\overline{\omega}_{\rm D}$.] Assuming $\omega_{\rm D}=\omega_{\rm H}/\sqrt{2}$ for both the *t* and *o* sites, Eq. (1) becomes

$$\Delta E_{\rm vib}=\frac{3}{2}\hbar\left\{1-\frac{1}{\sqrt{2}}\right\}(\omega_{\rm H}^{o}-\omega_{\rm H}^{t})\approx-0.44\hbar(\omega_{\rm H}^{t}-\omega_{\rm H}^{o}). \tag{2}$$

Hence, since *t*-site frequencies are larger than *o*-site frequencies, such transpositions of H_t and D_o atoms will lower the total vibrational energy of the system. Yet, such energy-lowering contributions to the free energy are offset by decreases in the configurational entropy, since in effect, the direction of these isotopic transpositions causes the system to become more isotopically ordered. Thus, the resulting isoto-

pic distributions will be determined by a temperature-dependent balance between the enthalpic and entropic contributions to the free energy.

It is useful to generalize the thermodynamic treatment of $Ce(H_{0.33}D_{0.67})_3$ by Somenkov *et al.*,[5] to describe the isotope-related perturbations to the free energy associated with the arbitrary fcc-based rare-earth hydride system $R(H_yD_{1-y})_{2+x}$ having an H/(H+D) isotopic mole fraction y and an (H+D)/R stoichiometric ratio $2+x$. In the simplest derivation, we assume that (i) the *t*-site sublattice is completely filled, so that all $(1-x)$ interstitial vacancies are part of the *o*-site sublattice, (ii) the *t*-site sublattice is an ''ideal solution'' of H and D while the *o*-site sublattice is an ''ideal solution'' of H, D, and vacancies, and (iii) metal-hydrogen and hydrogen-hydrogen interactions are isotope independent.

Within this approach, one can define the molar free energy $F=E-TS$ as a function of f_H, the isotopic atom fraction of H in the *o*-site sublattice. Thus, for $R(H_yD_{1-y})_{2+x}$, the molar enthalpy and entropy can be described by

$$E=E_0+xNf_H\Delta E_{vib} \tag{3}$$

and

$$S=S_0+S_{conf}=S_0+k\ln(\Omega_t\Omega_o), \tag{4}$$

where E_0 and S_0 are constants, N is Avogadro's number, xNf_H is the equilibrium number of H_o atoms per mole $R(H_yD_{1-y})_{2+x}$, ΔE_{vib} is the vibrational energy change per $H_t \rightleftharpoons D_o$ atom transposition as defined by Eq. (2), S_{conf} is the molar configurational entropy contribution, k is Boltzmann's constant, Ω_t is the number (per mole) of physically distinct *t*-site arrangements of H_t and D_t atoms, and Ω_o is the number (per mole) of physically distinct *o*-site arrangements of H_o and D_o atoms and vacancies. The latter two quantities can be defined as

$$\Omega_t=\frac{N_t!}{N_{H_t}!N_{D_t}!}=\frac{(2N)!}{\{N(2y+xy-xf_H)\}!\{N(2-2y-xy+xf_H)\}!} \tag{5}$$

and

$$\Omega_0=\frac{N_o!}{N_{H_0}!N_{D_o}!N_{\nu_o}!}=\frac{N!}{(Nxf_H)!\{Nx(1-f_H)\}!\{N(1-x)\}!}, \tag{6}$$

where the N_i's refer to the numbers (per mole) of i sites, atoms, and vacancies. Substituting these expressions for Ω_t and Ω_o into Eq. (4) and simplifying by Stirling's theorem yields

$$\begin{aligned}S(f_H)=S_0+Nk\{&2\ln 2-(2y+xy-xf_H)\ln(2y+xy-xf_H)\\&-(2-2y-xy+xf_H)\ln(2-2y-xy+xf_H)\\&-xf_H\ln(xf_H)-x(1-f_H)\ln[x(1-f_H)]\\&-(1-x)\ln(1-x)\}.\end{aligned} \tag{7}$$

Substituting the expressions for $E(f_H)$ [Eq. (3)] and $S(f_H)$ [Eq. (7)] into the free-energy relation and differentiating with respect to f_H yields

$$\frac{\partial F}{\partial f_H}=xN\left\{\Delta E_{vib}-kT\ln\left[\frac{(1-f_H)(2y+xy-xf_H)}{f_H(2-2y-xy+xf_H)}\right]\right\}. \tag{8}$$

The free energy is minimized when $\partial F/\partial f_H=0$. This condition leads to a general relationship between ΔE_{vib} and f_H, where

$$\Delta E_{vib}=kT\ln\left[\frac{(1-f_H)(2y+xy-xf_H)}{f_H(2-2y-xy+xf_H)}\right]. \tag{9}$$

Since it is common for the H_o atoms in superstoichiometric rare-earth dihydrides to undergo *o*-site sublattice structural ordering as the temperature decreases,[6] one must consider the effect of this ordering on the vibrational-energy change ΔE_{vib} in Eq. (3) and the configurational entropy contribution S_{conf} in Eq. (4). Since order-induced changes to the vibrational density of states for the fcc-based rare-earth hydrides appear to be minor,[3,4] associated changes in ΔE_{vib} are expected to be insignificant and can be ignored. As for the concomitant configurational entropy changes, one can assume that full *o*-site sublattice ordering reduces the number of available *o* sites N_o to xN in Eq. (6) and eliminates the $N_{\nu_o}!$ vacancy term, since H_o and D_o atoms are restricted to their ordered sublattice positions. Despite these changes to Eq. (6), the resultant expression for ΔE_{vib} is found to remain unmodified from that assuming a disordered *o*-site sublattice. Hence, to a first approximation, the temperature-dependent degree of *o*-site sublattice ordering does not significantly affect the generality of Eq. (9).

EXPERIMENTAL DETAILS

Both La- and Tb-based hydrides were synthesized by reaction of the metals with H_2 and/or D_2, as discussed elsewhere.[1] To minimize the problems associated with sample impurities, only high-purity (99.99% atomic fraction) metals and research grade H_2 and D_2 gases were used. For these superstoichiometric β-phase samples, the pure baseline dihydride or dideuteride was always formed first by evacuating any excess H or D above $x=2$ at 773 K, followed by adjustments in the stoichiometry by reaction with additional H_2 or D_2. Samples containing both hydrogen isotopes were synthesized using gas mixtures in the appropriate isotopic ratio.

The neutron scattering experiments were performed at the NIST Center for Neutron Research at the National Institute of Standards and Technology. Neutron-powder-diffraction measurements were made using the BT-1, 32-detector, high-resolution, powder diffractometer[7] with the Cu(311) monochromator at a wavelength of 1.5391(1) Å and horizontal divergences of 15′, 20′, and 7′ of arc for the in-pile, monochromatic-beam, and diffracted-beam collimators, respectively. All refinements were carried out with the Rietveld method[8] using the program GSAS.[9] Neutron-scattering amplitudes used in the refinements were 8.27, 7.38, 6.67, and −3.74 fm for La, Tb, D, and H, respectively.[9]

Neutron-vibrational-spectroscopy measurements were

made using the BT-4 filter-analyzer spectrometer[10] with the Cu(220) monochromator. The high-resolution Be-graphite-Be filter analyzer with an assumed final energy of 1.2 meV was used for the La-based compounds. Horizontal collimations before and after the monochromator were 40′ and 20′ of arc, respectively. The low-resolution Be filter analyzer with an assumed final energy of 3.0 meV was used for the Tb-based compounds. In this configuration, horizontal collimations before and after the monochromator were 40′ and 40′ of arc, respectively. The energy-dependent resolution (full width at half maximum) associated with a particular spectrum is denoted by horizontal bars beneath the peaks. Relative spectral scale factors for different samples in the figures are chosen so as to aid in lineshape comparisons, and spectral lines are drawn only as guides to the eye.

RESULTS AND DISCUSSION

A variety of NVS and NPD measurements were performed on the mixed-isotope system $La(H_yD_{1-y})_{2.50}$ (i.e., $x=0.5$) for $0 \leqslant y \leqslant 1$. Previous NPD measurements[11] have indicated that $LaD_{2.50}$ transforms from cubic ($Fm3m$) to tetragonal ($I4_1/amd$) symmetry below ≈385 K accompanied by the onset of long-range D ordering in the *o*-site sublattice. The D_o ordering is complete by ≈250 K and can be described as a repeating sequence of four (042) *o*-site planes comprised of two adjacent filled planes followed by two adjacent empty planes. Figure 1 displays the neutron vibrational spectra for $LaD_{2.50}$ (i.e., $y=0$) and $LaH_{2.50}$ (i.e., $y=1$), confirming the qualitative similarity of the low-temperature D and H optic-vibrational density of states. The fundamental D_o and H_o vibrational-energy bands are centered near 51.5 and 71.5 meV, respectively. The next three higher-energy vibrational bands in each spectrum are primarily associated with the D_t and H_t atoms, with only minor contributions from D_o and H_o overtone (i.e., $\nu=0\rightarrow 2$) bands evident as high-energy shoulders near 103 and 143 meV, respectively. In addition, the $LaD_{2.50}$ spectral features above 125 meV are due to D_t overtone bands. The complexity of all vibrational bands is a manifestation of significant phonon dispersion effects due to D-D and H-H interactions.[1,2] The comparison of the 10 and 300 K spectra for $LaH_{2.50}$ confirms only minor qualitative changes in the phonon bands with changes in the degree of H_o sublattice order. Since the lowest overtone energy of 103 meV (occurring in the case of $LaD_{2.50}$) corresponds to a vibrational temperature of about 1200 K (threefold higher than the maximum temperature of 400 K used in this study), the vast majority of H and D atoms in the mixed-isotope samples were indeed in their ground-state levels during the NPD and NVS measurements.

Because of the significant phonon dispersion effects in this system, the value for $\Delta E_{\rm vib}$ was estimated from Eq. (1) using the mean fundamental vibrational energies $\hbar\overline{\omega}_{\rm H}$ and $\hbar\overline{\omega}_{\rm D}$ for H and D in the *t* and *o* sites as determined from the low-temperature NVS data in Fig. 1. NVS data taken with a filter-analyzer spectrometer represent a reasonable approximation of the hydrogen vibrational density of states.[10] For hydrides of a relatively heavy element such as La (or Tb), the contributions from optoacoustic multiphonon sidebands are small at low temperature and were ignored in the $\hbar\overline{\omega}_{\rm H}$ and $\hbar\overline{\omega}_{\rm D}$ calculations. After estimating and removing the high-energy shoulders due to the D_o and H_o overtone bands, we performed minor intensity corrections to the resulting spectra by dividing each fundamental band by the appropriate Debye-Waller factor $\exp(-\alpha Q^2)$, where Q is the momentum transfer, $\alpha=B/(8\pi^2)$, and B is the isotropic temperature factor for the vibrating atoms. For $LaD_{2.50}$ at 10 K, NPD data[11] yield B values of ≈2 and 1 Å^2 for the D_o and D_t atoms, respectively. Making a harmonic approximation, the B values for the H_o and H_t atoms were assumed to be twice as large as those of their D counterparts. Such spectral adjustments resulted in a value of $\Delta E_{\rm vib}=-19(1)$ meV.

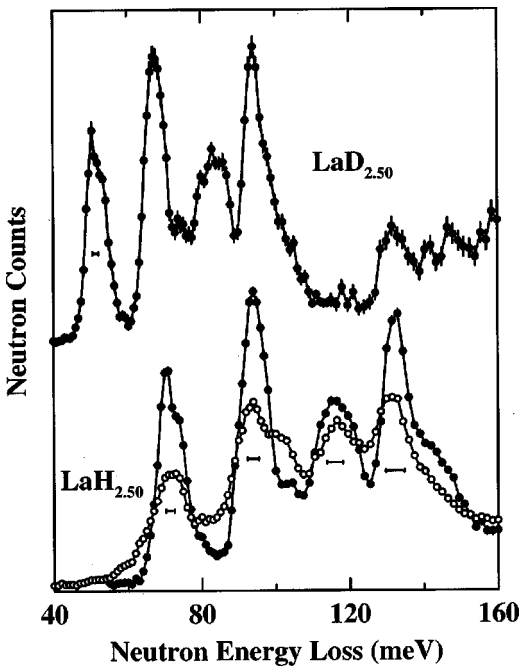

FIG. 1. Neutron vibrational spectra of $LaD_{2.50}$ and $LaH_{2.50}$ at 10 K (closed circles) and 300 K (open circles). The $LaD_{2.50}$ spectrum was renormalized to display vibrational peaks with intensities comparable to those of the $LaH_{2.50}$ spectra.

A second mixed-isotope system of nominal stoichiometry $Tb(H_{0.1}D_{0.9})_{2.25}$ [but with a Rietveld-refined stoichiometry $Tb(H_{0.1}D_{0.9})_{2.22}$; see below] was also investigated to further test the applicability of Eq. (9) to a different rare-earth hydride system and stoichiometry. According to NPD measurements,[12,13] $TbD_{2.25}$ transforms from D_o-disordered cubic ($Fm3m$) symmetry to a D_o-ordered tetragonal ($I4/mmm$) symmetry below ≈330 K,[14] similar to the structural behavior of $LaD_{2.25}$.[15] The D_o ordering is complete by ≈270 K (Ref. 14) and can be described as a repeating sequence of four (042) *o*-site planes comprised of one filled plane followed by three adjacent empty planes. Figure 2 illustrates the neutron vibrational spectra for $TbD_{2.25}$ and $TbH_{2.25}$. The relatively smaller lattice constants for the Tb-based system compared to the La-based system results in relatively higher energies by ≈20% for the phonon bands associated with the *o*- and *t*-site hydrogen isotopes. The D_o and H_o overtone bands are evident as high-energy shoulders near 119 and 165 meV, respectively, whereas the D_t overtone bands are located above 145 meV. Similar to $LaH_{2.50}$, the spectra for $TbH_{2.25}$ indicate qualitatively little change going from low temperature (4.2 K) to high temperature (297

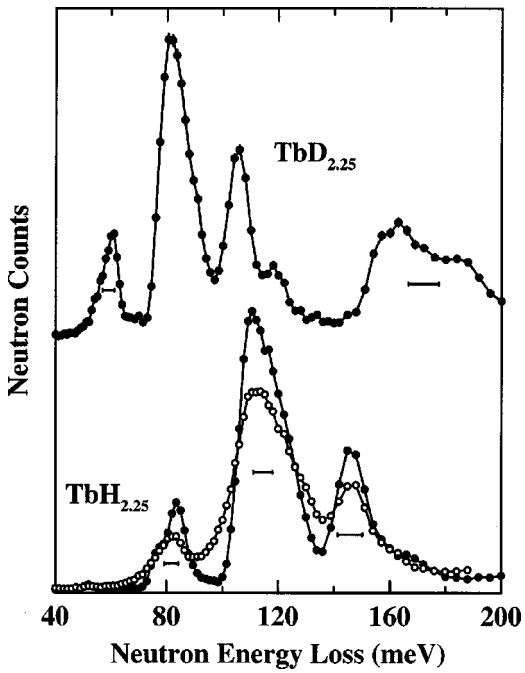

FIG. 2. Neutron vibrational spectra of $TbD_{2.25}$ and $TbH_{2.25}$ at 4.2 K (closed circles) and 297 K (open circles). The $TbD_{2.25}$ spectrum was renormalized to display vibrational peaks with intensities comparable to those of the $TbH_{2.25}$ spectra.

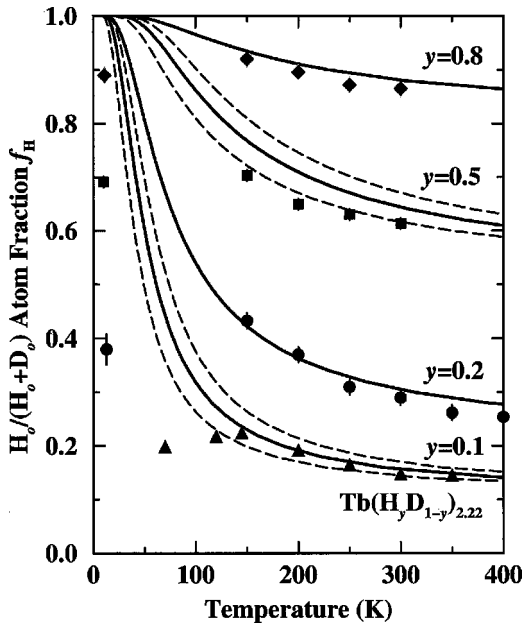

FIG. 3. Temperature dependence of f_H for $La(H_yD_{1-y})_{2.50}$ compounds ($y=0.2$, 0.5, and 0.8) and $Tb(H_{0.1}D_{0.9})_{2.22}$ as determined by Rietveld-refined models of NPD patterns. Solid lines represent the temperature dependence of f_H predicted from Eq. (9) using the ΔE_{vib} values estimated from the NVS data in Figs. 1 and 2. ($\Delta E_{vib}=-19$ and -15 meV for the La and Tb compounds, respectively.) Dashed lines bracketing the solid lines for $La(H_{0.5}D_{0.5})_{2.50}$ and $Tb(H_{0.1}D_{0.9})_{2.22}$ represent solutions of Eq. (9) for 20% larger (upper lines) and 20% smaller (lower lines) ΔE_{vib} values.

K). Again, because of significant phonon dispersion effects, ΔE_{vib} was estimated from the low-temperature NVS data in Fig. 2. Similar Debye-Waller-factor adjustments to the spectra using 70-K B values determined by NPD (Ref. 13) of ≈ 1.4 and 1 Å^2 for the D_o and D_t atoms, respectively, and twofold larger values for the corresponding H_o and H_t atoms yielded a ΔE_{vib} value of $-15(1)$ meV.

The data points in Fig. 3 represent the temperature-dependent values of f_H as determined by Rietveld refinements of NPD patterns from $La(H_yD_{1-y})_{2.50}$ for $y=0.2$, 0.5, and 0.8, as well as from $Tb(H_{0.1}D_{0.9})_{2.25}$ (i.e., $y=0.1$). In all these mixed-isotope refinements, the degree of o-sublattice order at each temperature, as reflected by the various interstitial o-site occupancies, was fixed at the values determined by Rietveld refinements of patterns from pure deuteride samples. The relative isotopic abundances associated with the o and t sites were refined as free parameters. Good fits resulted in all cases, and the y values as determined from sample preparation were consistently in agreement with the total isotopic abundances determined from the refinements. Refinements for the La-based compounds confirmed the value of x determined from sample preparation. Similar refinements for $Tb(H_{0.1}D_{0.9})_{2.25}$ consistently underestimated the nominal value of $x=0.25$ determined via synthesis; i.e., we obtained values in the range of 0.218–0.225 over the temperature span measured. Yet, this is in line with our previously reported 70-K value of $x=0.233(5)$ for a sample with a nominal stoichiometry of $TbD_{2.25}$ (Ref. 13) as well as the phase-boundary values of $x_{max}\approx 0.22-0.23$ found from our refinements of NPD data for the two-phase $TbD_{2.35}$ compound.[14] Although no effort was made to perform NPD measurements on the $TbH_{2.25}$ sample, the value of $x_{max}\approx 0.25$ reported elsewhere for TbH_{2+x} (Ref. 6) suggests that x_{max} may well be isotope dependent and ≈10% smaller for the deuterided compound. This would be consistent with the observed isotope-dependent differences in lattice constants for superstoichiometric rare-earth dihydride samples, with the lattices of RH_{2+x} being slightly larger than those of the comparable RD_{2+x}.[6] Increasing the value of x in these compounds causes a lattice contraction, presumably to increase the energy-stabilizing interaction of the additional electron and the metal d potential.[16] Hence, if the γ (trihydride) phase becomes more stable than the β phase at some limiting lattice size, the corresponding value of x_{max} will indeed tend to be larger for hydrides than deuterides. Based on the Rietveld refinements, we chose to assume that the mixed-isotope $Tb(H_{0.1}D_{0.9})_{2.25}$ sample had a β-phase stoichiometry of $Tb(H_{0.1}D_{0.9})_{2.22}$ (as labeled in Fig. 3), with the excess H and D present as part of an additional, insignificant, mixed-isotope trihydride phase.

The lines in Fig. 3 represent the predicted temperature dependence using Eq. (9) with the values of ΔE_{vib} determined from the NVS data. For example, for $La(H_yD_{1-y})_{2.50}$ with $y=0.2$, Eq. (9) becomes

$$\Delta E_{vib}=-19\,\text{meV}=kT\ln\left[\frac{(1-f_H)^2}{f_H(3+f_H)}\right]. \qquad (10)$$

Figure 4 depicts the theoretical equilibrium structures for $La(H_{0.2}D_{0.8})_{2.50}$ at 0 K, where complete isotopic order ($f_H=1$) occurs, and at high temperature ($T\rightarrow\infty$), where complete isotopic disorder ($f_H=0.2$) occurs. Since the discrepancies in β-phase stoichiometries for the Tb-based compounds were small, the ΔE_{vib} value of -15 meV determined from the vibrational spectra of the nominal $TbD_{2.25}$ and

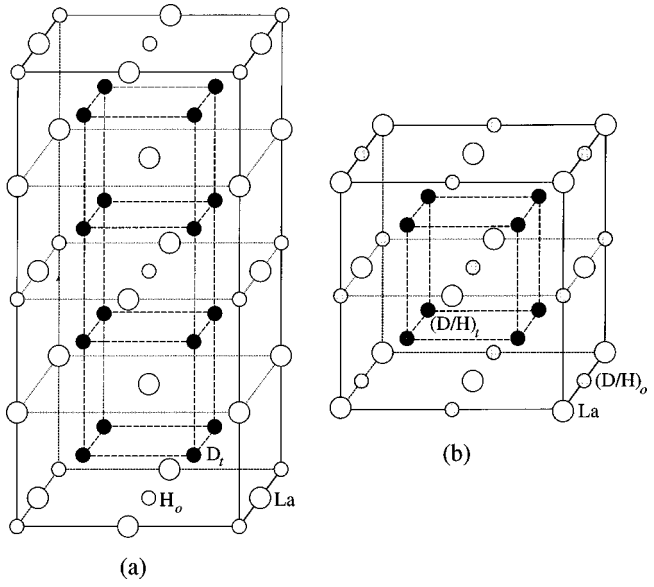

FIG. 4. Theoretical equilibrium structures of $La(H_{0.2}D_{0.8})_{2.50}$ at (a) 0 K showing complete isotopic order and (b) $T\rightarrow\infty$ showing complete isotopic disorder. The low-temperature phase possesses a structural order within the *o*-site sublattice as described in the text, whereas the high-temperature phase possesses a structural disorder with each *o* site statistically half-occupied.

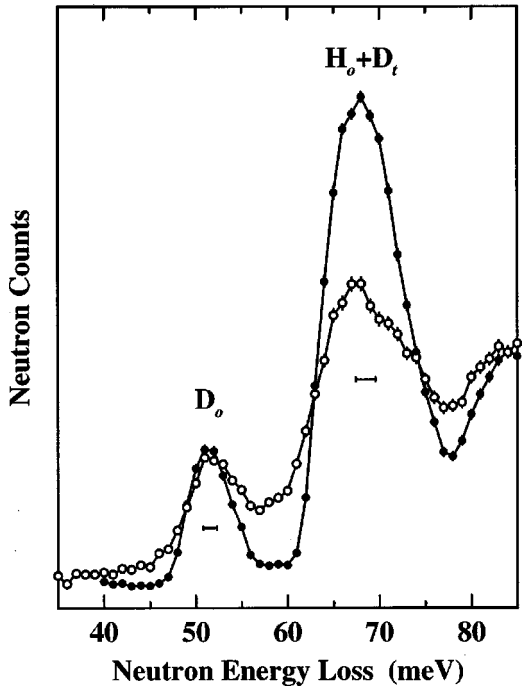

FIG. 5. Neutron vibrational spectra of $La(H_{0.2}D_{0.8})_{2.50}$ at 10 K (closed circles) and 300 K (open circles) in the region of the H_o and D_o vibrational-mode energies.

$TbH_{2.25}$ compounds was used without further corrections in Eq. (9) to predict the temperature-dependent isotopic arrangements for $Tb(H_{0.1}D_{0.9})_{2.22}$. The dashed lines bracketing the solid lines for $La(H_{0.5}D_{0.5})_{2.50}$ and $Tb(H_{0.1}D_{0.9})_{2.22}$ represent solutions of Eq. (9) for $\pm 20\%$ deviations in the $\Delta E_{\rm vib}$ values, illustrating the sensitivity of $f_{\rm H}$ to changes in $\Delta E_{\rm vib}$.

Reasonable agreement is observed between theory and experiment in Fig. 3 for all samples above $\approx$150 K. Below this temperature, the data indicate no change in $f_{\rm H}$ suggesting that the H and D mobilities are significantly reduced, presumably due to a relatively large activation energy barrier associated with $t\rightarrow o$ jumps of the H and D atoms. In particular, the degree of isotopic order that is present just above 150 K becomes essentially ''frozen in'' as the temperature is lowered further. Hence, below $\approx$150 K, the predicted increase in isotopic order with decreasing temperature is kinetically forbidden over the timescale of the experiments. This is consistent with what Somenkov *et al.*[5] observed for $Ce(H_{0.33}D_{0.67})_3$, where the isotopic order at 4.8 and 78 K was unchanged and substantially below the predicted value. This is also in line with TbH_{2+x} resistivity data,[17] which reflected a lack of H mobility below $\approx$165 K.

Although the overall agreement is reasonable in Fig. 3, the observed small deviations are not unexpected in light of the simplifying assumptions made. For example, the lattice constants of the mixed-isotope and corresponding single-isotope compounds are not truly identical. Debye-Waller factors for the H-derived compounds are not known accurately. Moreover, because of hydrogen-hydrogen interactions, the H and D vibrational densities of states are somewhat affected by isotopic mixing. These interactions also mean that there are probably no entirely pure *o*-site or *t*-site vibrational modes; i.e., there will be some contribution of *o*-site hydrogen to *t*-site modes and vice versa. This latter factor, in particular, most likely causes the tendency of the theoretical lines in Fig. 3 to slightly overestimate the measured isotopic separations above 150 K; i.e., the presence of such partial mode mixing of *o*-site and *t*-site atoms translates into an artificially high $\Delta E_{\rm vib}$ value as calculated assuming unmixed vibrational bands of the single-isotope compounds. Yet, the experimental results suggest that these and all other compromising factors are indeed minor perturbations.

Besides the NPD results, NVS data for mixed-isotope hydrides also corroborate the occurrence of temperature-dependent isotopic ordering. This is exemplified in Fig. 5, which illustrates the vibrational energy region of the H_o and D_o atoms in $La(H_{0.2}D_{0.8})_{2.50}$ at 10 and 300 K. A comparison of the 10-K vibrational spectrum for $La(H_{0.2}D_{0.8})_{2.50}$ with those for $LaH_{2.50}$ and $LaD_{2.50}$ in Fig. 1 indicates that the band near 51.5 meV is due solely to D_o vibrations, whereas the band near 68 meV is due mainly to H_o vibrations with a minor contribution from overlapping D_t vibrations in this region. Despite the complication from D_t vibrations and the expected spectral attenuations with increased temperature, it is clear from the relative integrated intensity changes of the H_o and D_o vibrational bands that the H_o/D_o ratio decreases upon increasing the temperature from 10 to 300 K.

For a more quantitative analysis of these changes, we compared the decrease in the H_o/D_o atom ratio as determined by Rietveld refinements of the NPD data to the observed decrease in the H_o/D_o vibrational intensity ratio as determined from the spectra in Fig. 5. According to the NPD refinement results, the H_o/D_o atom ratio for $La(H_{0.2}D_{0.8})_{2.50}$ is $\approx 0.38/0.62 = 0.61$ at 10 K and $\approx 0.29/0.71 = 0.41$ at 300 K, indicating that the ratio is a factor of $0.61/0.41 = 1.5$ larger at 10 K. These H_o/D_o ratios correspond to H_t/D_t ratios of $\approx 0.16/0.84 = 0.19$ at 10 K and $\approx 0.18/0.82 = 0.22$ at 300 K. For the $LaD_{2.50}$ spectrum at 10 K in Fig. 1, we observed a D_t/D_o intensity ratio of 1.05 for the lowest-energy D_t band

near 67.5 meV and the D_o band near 51.5 meV. We used this ratio as a starting point for estimating how much scattering intensity to subtract from the 68-meV features in Fig. 5 due to the D_t contributions, thus ending up with the amount of scattering intensity due solely to the H_o vibrations. Since the NPD data indicated that the D_o atom fraction is not the same as the D_t atom fraction for $La(H_{0.2}D_{0.8})_{2.50}$ at either 10 or 300 K, we had to correct the D_t/D_o intensity ratio derived from the $LaD_{2.50}$ spectrum to reflect this fact. In particular, we used the NPD-derived isotopic atom fractions of D in the *t* and *o* sites of 0.84 and 0.62, respectively, at 10 K, and 0.82 and 0.71, respectively, at 300 K to adjust the $LaD_{2.50}$-derived D_t/D_o intensity ratio by a factor of $0.84/0.62=1.35$ at 10 K and $0.82/0.71=1.15$ at 300 K. Next, after determining the integrated intensities of the $La(H_{0.2}D_{0.8})_{2.50}$ vibrational bands in Fig. 5, we used the corrected D_t/D_o intensity ratios in conjunction with the intensities of the D_o vibrational bands to estimate and subtract the intensity contributions of the overlapping D_t bands from the H_o-dominated bands. The H_o/D_o intensity ratios calculated from these corrections at each temperature indicated that the H_o/D_o atom ratio was a factor of 1.5 larger at 10 K than at 300 K, in excellent agreement with the NPD results.

CONCLUSIONS

The NPD and NVS results for the fcc-based, mixed-isotope, rare-earth hydrides $La(H_yD_{1-y})_{2.50}$ $(0\leqslant y\leqslant 1)$ and $Tb(H_{0.1}D_{0.9})_{2.22}$ are consistent with previous NPD measurements for $Ce(H_{0.33}D_{0.67})_3$ that suggested preferential isotopic occupation of H in the *o* sites and D in the *t* sites. The degree of isotopic separation is found to increase with decreasing temperature, presumably driven by the differences in the zero-point energies of H and D in the different interstitial sites. Decreasing the temperature below $\approx$150 K leads to a ''freezing in'' of the 150-K H and D lattice configuration, kinetically precluding further isotopic site separation at lower temperatures. These results confirm that isotopic site separation is a general phenomenon for fcc-based, mixed-isotope, rare-earth hydrides. Moreover, we believe that such behavior will occur in any metal-hydride system where there are significant differences in the zero-point energies associated with the different absorption sites. Once again, this type of study illustrates the unique capabilities of neutron scattering methods when used in combination with isotopically manipulated hydride samples.

*Also at the Department of Materials and Nuclear Engineering, University of Maryland, College Park, Maryland 20742.

[1] T. J. Udovic, J. J. Rush, and I. S. Anderson, J. Alloys Compd. **231**, 138 (1995).
[2] T. J. Udovic, J. J. Rush, Q. Huang, and I. S. Anderson, J. Alloys Compd. **253-254**, 241 (1997).
[3] T. J. Udovic, J. J. Rush, and I. S. Anderson, J. Phys.: Condens. Matter **7**, 7005 (1995).
[4] T. J. Udovic, Q. Huang, C. Karmonik, and J. J. Rush, J. Alloys Compd. **293-295**, 113 (1999).
[5] V. A. Somenkov, I. R. Entin, M. E. Kost, and S. Sh. Shil'shtein, Fiz. Tverd. Tela. (Leningrad) **17**, 2368 (1975) [Sov. Phys. Solid State **17**, 1563 (1975)].
[6] P. Vajda and J. N. Daou, in *Hydrogen Metal Systems I*, edited by F. A. Lewis and A. Aladjem (Scitec, Zurich, 1996), p. 71.
[7] J. K. Stalick, E. Prince, A. Santoro, I. G. Schroder, and J. J. Rush, in *Neutron Scattering in Materials Science II*, edited by D. A. Neumann, T. P. Russell, and B. J. Wuensch, MRS Symposia Proceedings No. 376 (Materials Research Society, Pittsburgh, PA, 1995), p. 101.
[8] H. M. Rietveld, J. Appl. Crystallogr. **2**, 65 (1969).
[9] A. C. Larson and R. B. Von Dreele, *General Structure Analysis System*, University of California, Berkeley, 1985.
[10] J. R. D. Copley, D. A. Neumann, and W. A. Kamitakahara, Can. J. Phys. **73**, 763 (1995).
[11] T. J. Udovic, Q. Huang, and J. J. Rush, J. Solid State Chem. **122**, 151 (1996).
[12] G. André, O. Blaschko, W. Schwarz, J. N. Daou, and P. Vajda, Phys. Rev. B **46**, 8644 (1992).
[13] Q. Huang, T. J. Udovic, J. J. Rush, J. Schefer, and I. S. Anderson, J. Alloys Compd. **231**, 95 (1995).
[14] T. J. Udovic and Q. Huang (unpublished).
[15] T. J. Udovic, Q. Huang, J. J. Rush, J. Schefer, and I. S. Anderson, Phys. Rev. B **51**, 12 116 (1995).
[16] Y. Wang and M. Y. Chou, Phys. Rev. B **49**, 10 731 (1994).
[17] P. Vajda, J. N. Daou, and J. P. Burger, Phys. Rev. B **36**, 8669 (1987).